Supplementary Information (SI) for Physical Chemistry Chemical Physics.

Supporting Information

Mechanistic insights into the inhibition of hIAPP fibrillation by amyloidogenic core-derived peptide NFGAILSS using computer simulations

Tanishka Mehta and Bhupesh Goyal*

Department of Chemistry & Biochemistry, Thapar Institute of Engineering & Technology, Patiala–147004, Punjab, India

*Corresponding author

Email: bhupesh@iitbombay.org; bhupesh@thapar.edu

List of contents

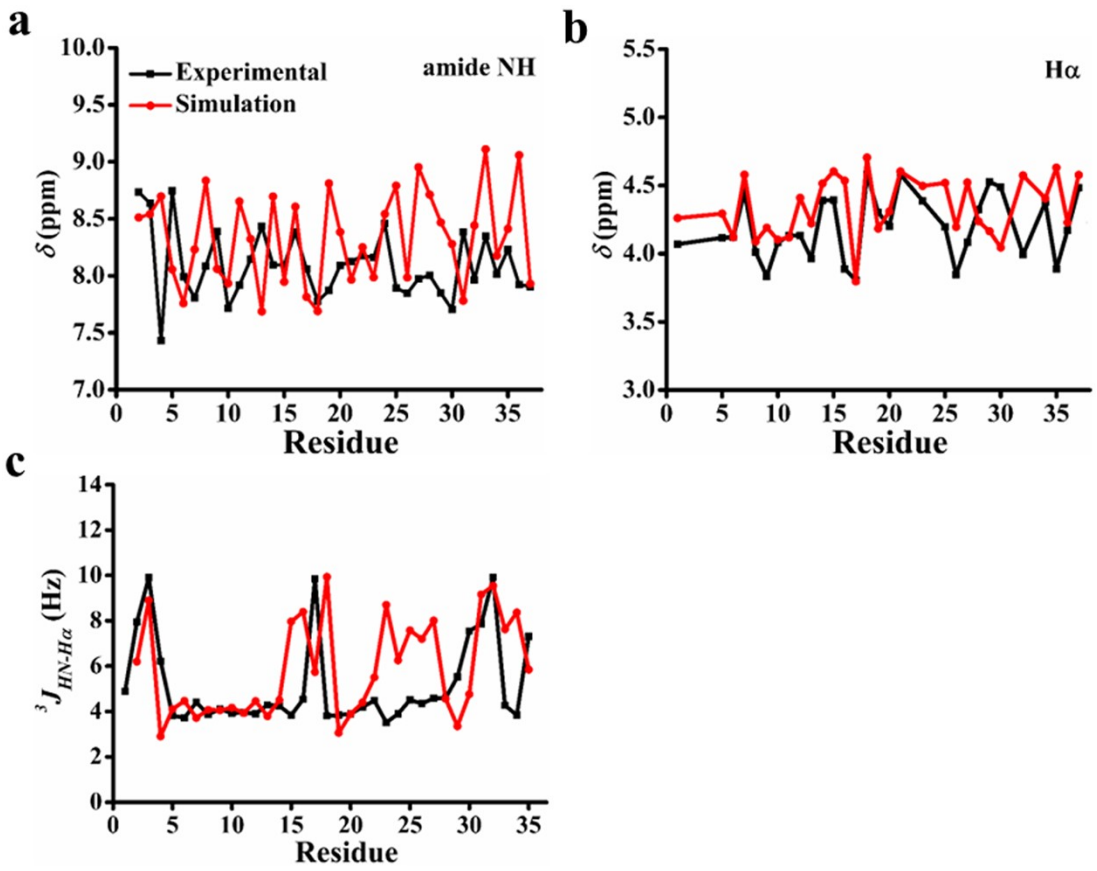

Fig. S1: Comparison of experimental and simulation NMR chemical shifts of amide NH and Hα atoms is shown in panels a and b, respectively. A comparison of the $^3J_{NH-H\alpha}$ coupling constant values of hIAPP residues evaluated for the experimental and simulation data is shown in panel c.

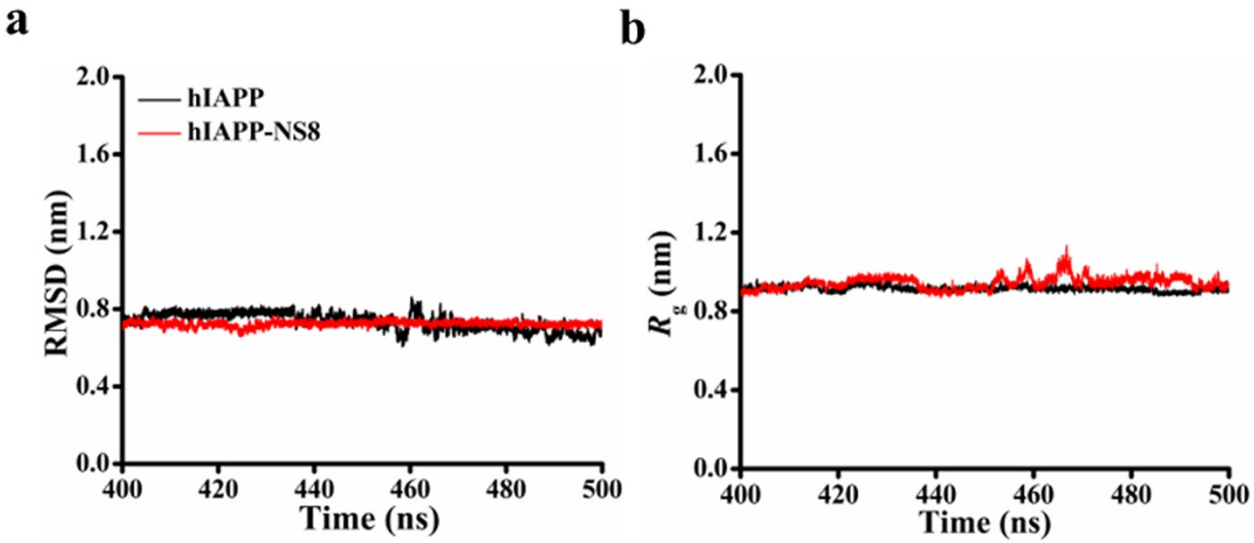

Fig. S2: Variations in the RMSD (panel a) and R_g (panel b) of hIAPP and hIAPP-NS8 complex during the last 100 ns of the simulation trajectory.

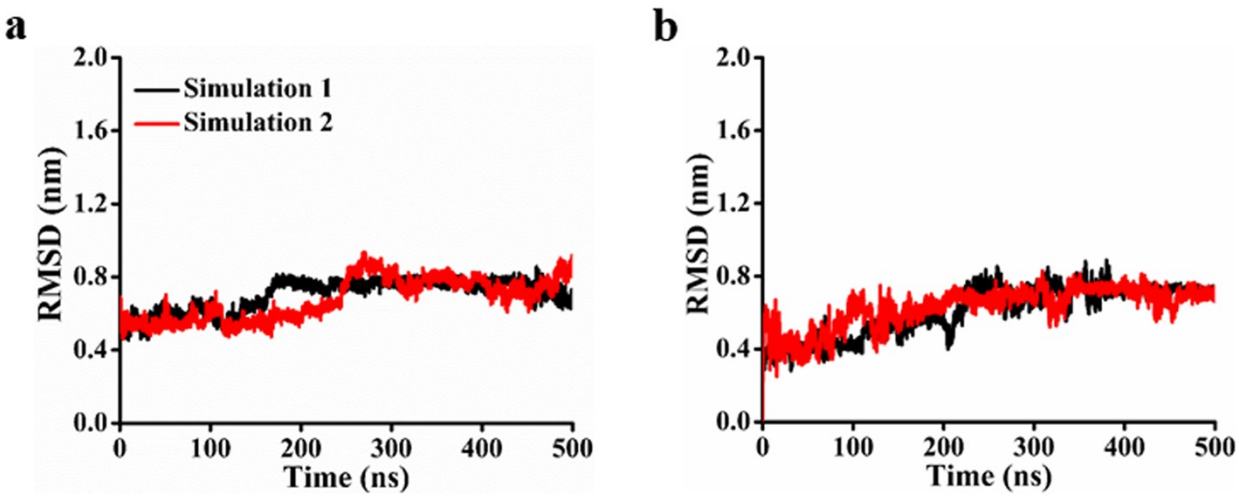

Fig. S3: Variations in the RMSD of hIAPP (panel a) and hIAPP-NS8 (panel b) for the repeat simulations with different initial velocities.

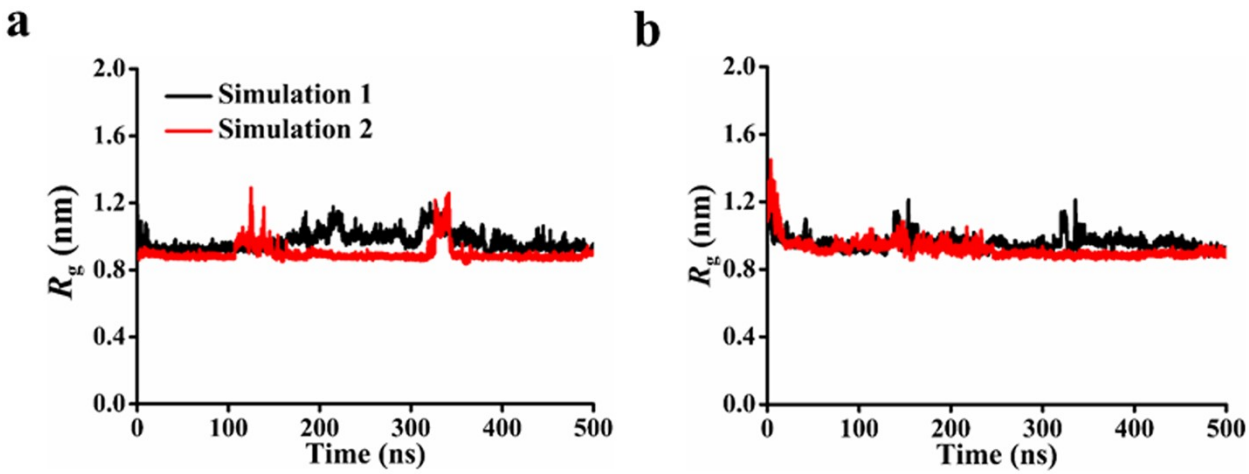

Fig. S4: Variations in the R_g of hIAPP (panel a) and hIAPP-NS8 (panel b) for the repeat simulations with different initial velocities.

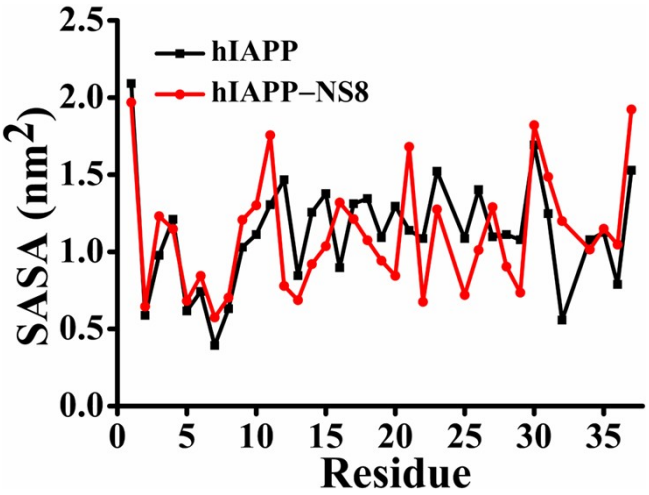

Fig. S5: NS8-mediated variations in the residue-wise SASA of hIAPP.

a

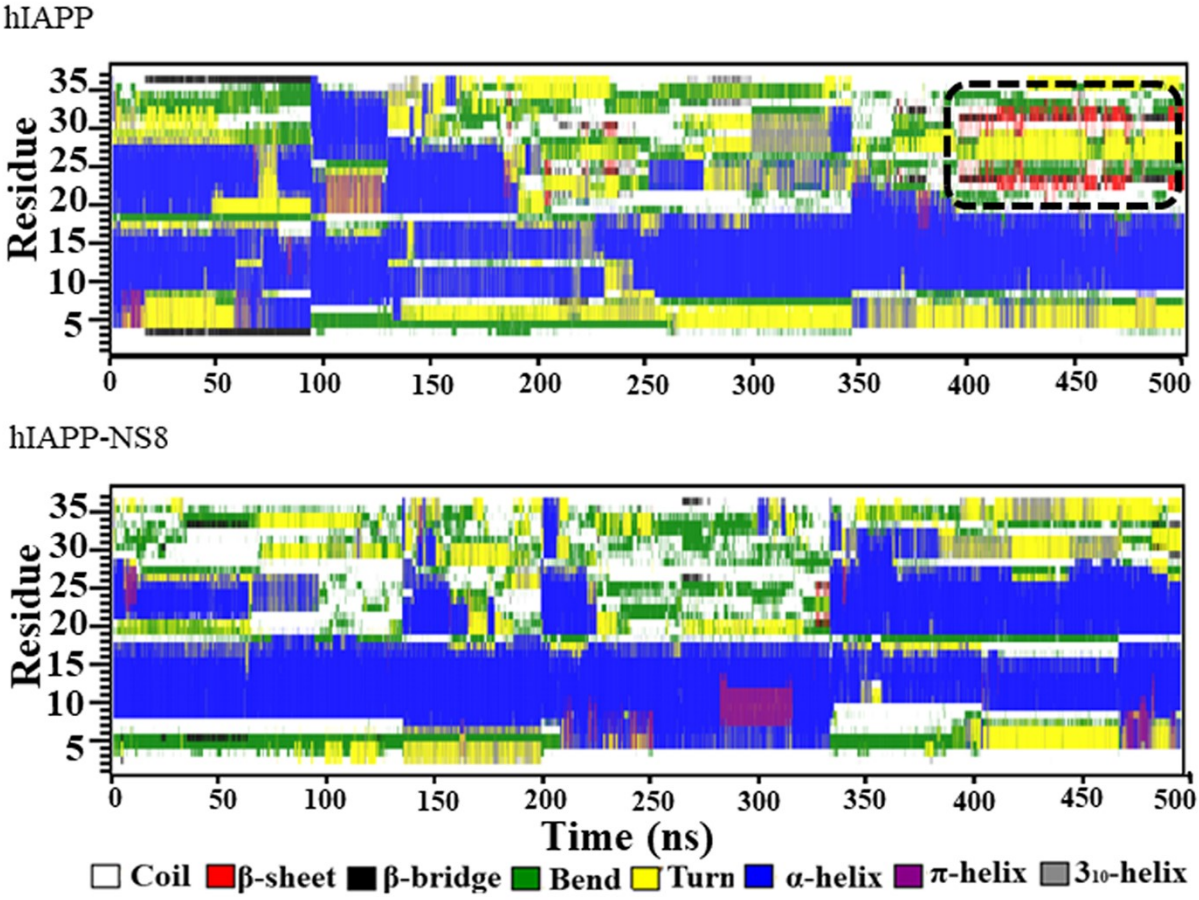

b

System	helix[a]	β-sheet[b]	bend	turn	coil
hIAPP	39.00 ± 1.95	7.00 ± 0.35	14.00 ± 0.70	18.00 ± 0.90	22.00 ± 1.10
hIAPP–NS8	43.00 ± 2.15	1.00 ± 0.05	13.00 ± 0.65	12.00 ± 0.60	31.00 ± 1.55

[a] helix is the sum of α–, π– and 3_{10} helix; [b] β–sheet is the sum of β–strand and β–bridge

Fig. S6: Sampling of various secondary structure elements in hIAPP and hIAPP-NS8 complex in the repeat simulations is shown in panel a. The influence of NS8 on the percentage composition of different secondary structure elements in hIAPP in the repeat simulations is listed in panel c.

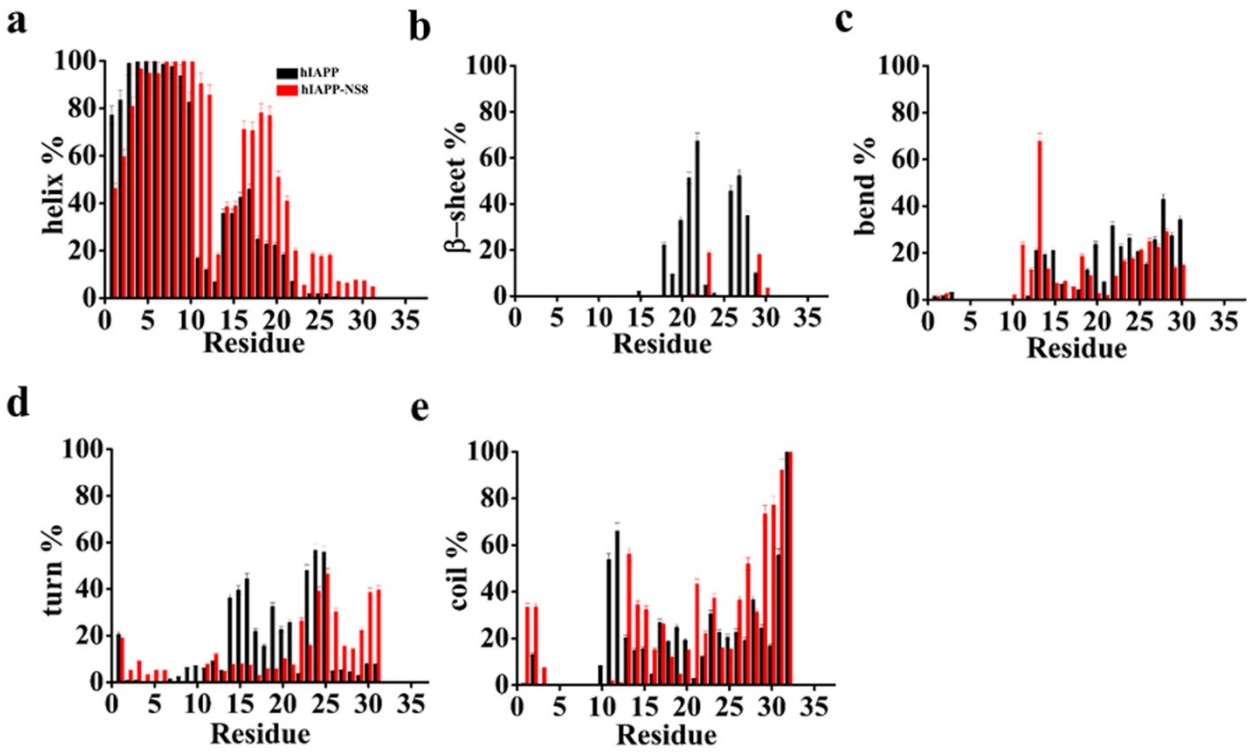

Fig. S7: NS8-induced residue-wise variations in the secondary structures of hIAPP.

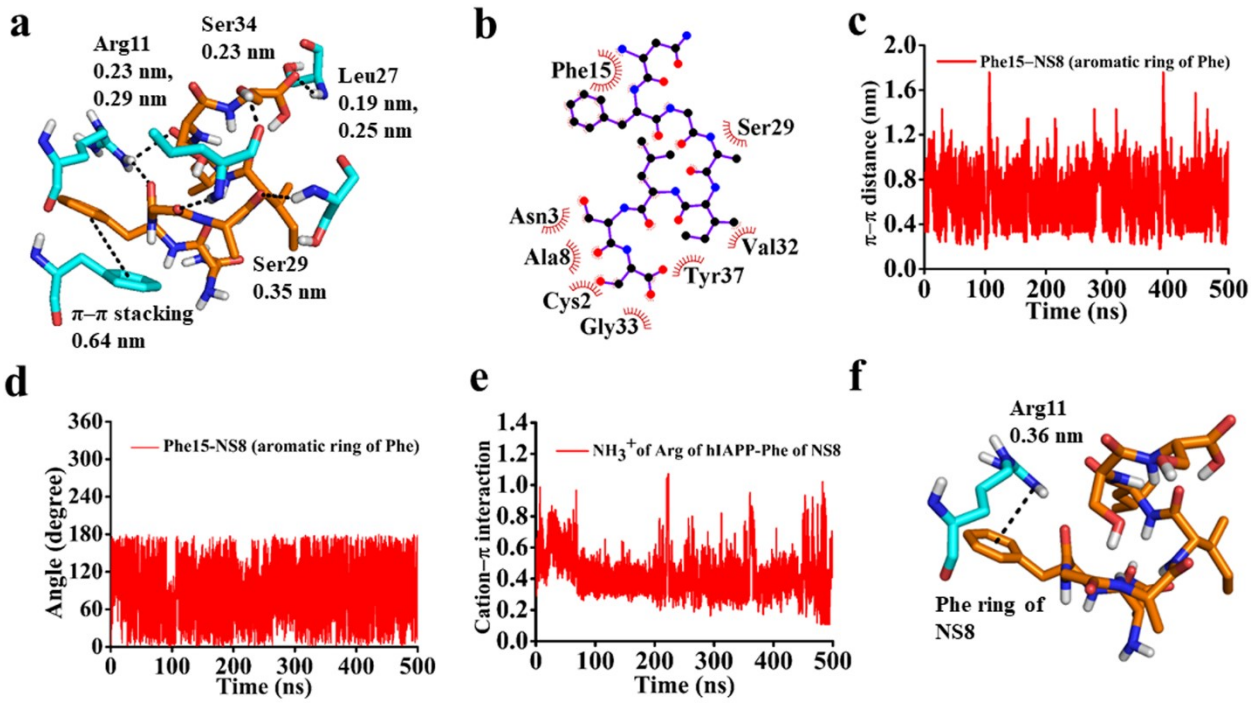

Fig. S8: Key interactions of NS8 with hIAPP in the illustrative conformation of the most-populated microstate of hIAPP (panel a). Hydrophobic contacts of NS8 with hIAPP in the illustrative conformation of the most-populated microstate (panel b). Variations in the COM distance between aromatic rings of Phe2 in NS8 and Phe15 of hIAPP with time (panel c). Variations in the angle between the aromatic planes of Phe2 in NS8 and Phe15 of hIAPP with time (panel d). Variations in the cation-π interaction distance between Arg11 of hIAPP and aromatic ring of Phe2 of NS8 (panel e). Conformational snapshot depicts cation-π interaction of NH_3^+ group of Arg11 of hIAPP with Phe2 of NS8 (panel f).

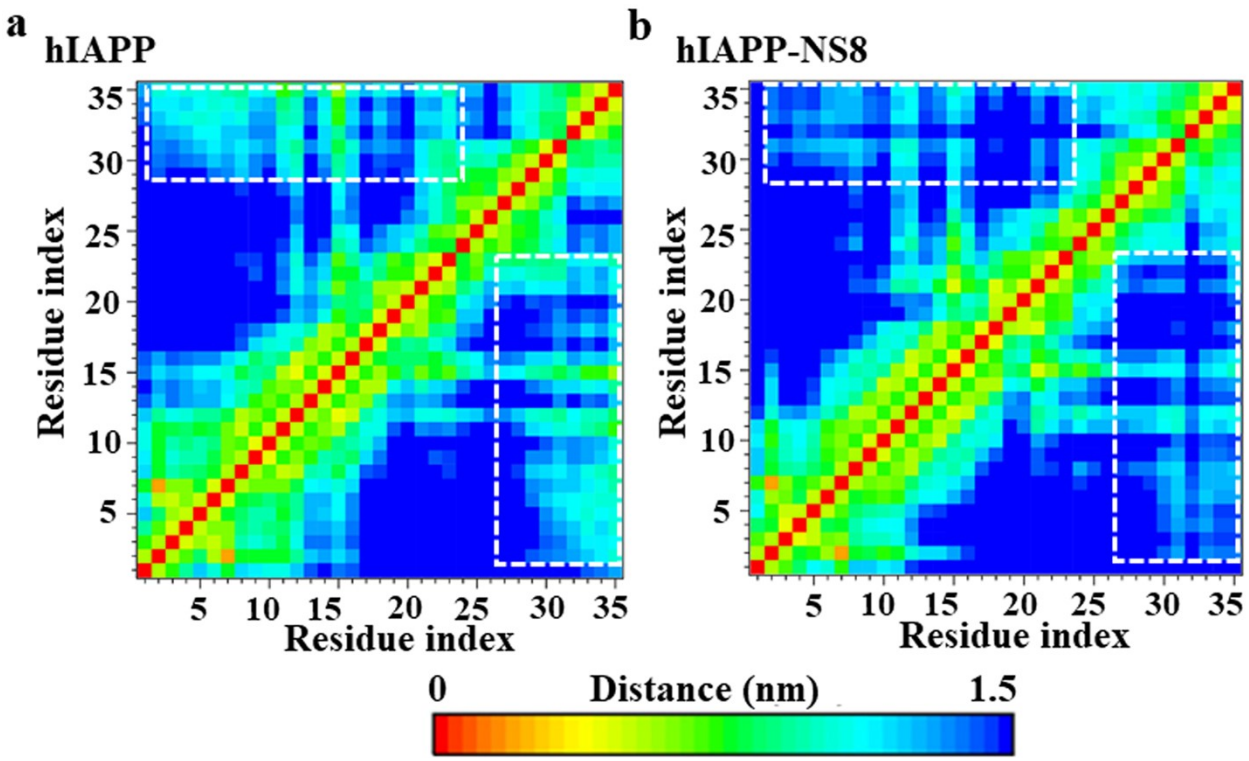

Fig. S9: Influence of NS8 on the intramolecular sidechain-sidechain contacts in hIAPP.

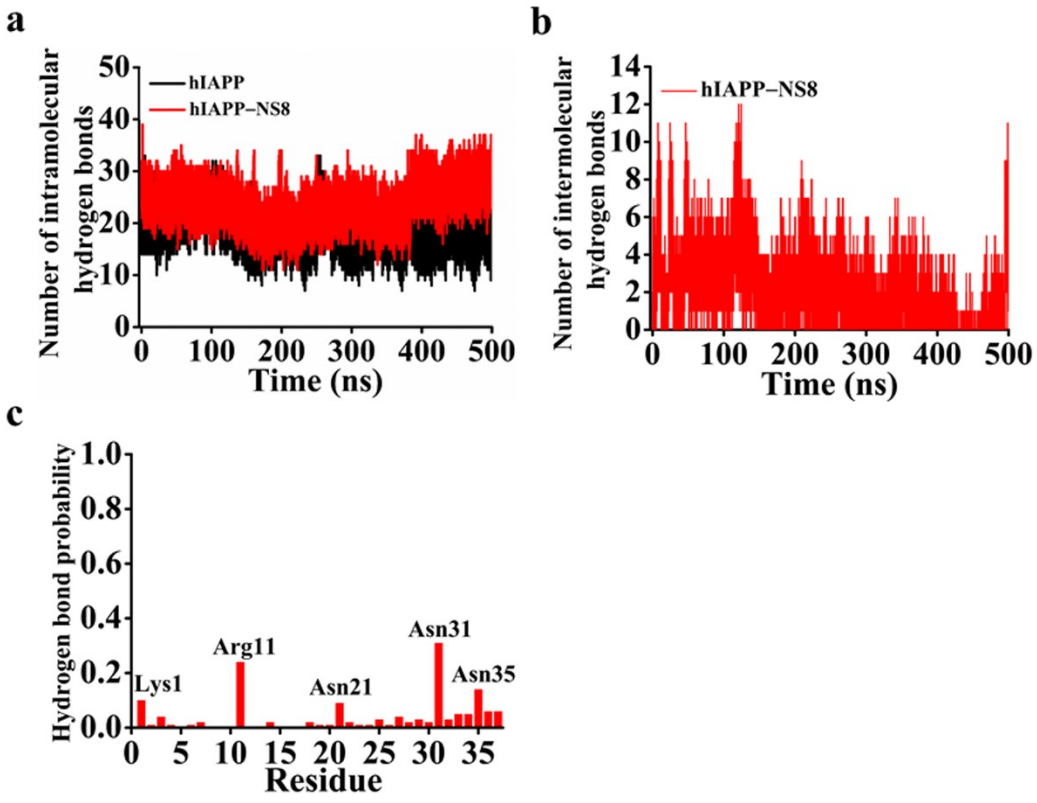

Fig. S10: NS8 modulates intramolecular hydrogen bonds in hIAPP (panel a). Intermolecular hydrogen bonds between hIAPP and NS8 during simulation (panel b). Hydrogen bond probability between hIAPP residues and NS8 during simulation (panel c).

Table S1: Molecular docking analysis of hIAPP-NS8 complex.

Peptide	AutoDock Vina binding energy (kcal/mol)	hIAPP residues participating in hydrogen bonds with NS8					hIAPP residues involved in hydrophobic contacts with NS8
		hIAPP		NS8		Distance (nm)	
NS8	–6.10	Asn3	(SC[a]: NH)	Ser8	(MC[b]:OC)	0.21	Lys1, Ala8,
		Arg11	(SC: NH1)	Ser8	(MC:OC)	0.21	Asn14, Phe15,
			(SC:NH2)	Ser8	(MC:OC)	0.25	Asn21, Asn22,
			(SC:NH)	Leu6	(MC:OC)	0.27	Ala25, Asn31,
			(SC:NH2)	Leu6	(MC:OC)	0.28	Ser34, Asn35
		Asn31	(MC: NH1)	Asn1	(SC:1HN)	0.34	
			(SC:CO)	Asn1	(SC:1HN)	0.27	
			(SC:CO)	Asn1	(SC:2HN)	0.30	
			(SC:CO)	Ala4	(SC:HN)	0.27	
			(SC:NH1)	Ile5	(MC:OC)	0.28	
			(SC:NH2)	Ile5	(MC:OC)	0.34	
		Asn35	(MC: NH1)	Asn1	(MC:OC)	0.32	

[a]SC: side chain; [b]MC: main chain

Table S2: RMSD and R_g values of hIAPP and hIAPP-NS8 systems for the whole simulation trajectory and the last 100 ns of the simulation trajectory.

System	Time (ns)	RMSD (nm)	R_g (nm)
hIAPP	0–500	0.70 ± 0.04	1.00 ± 0.05
	400–500	0.74 ± 0.02	0.96 ± 0.01
hIAPP-NS8	0–500	0.61 ± 0.03	0.93 ± 0.04
	400–500	0.72 ± 0.00	0.94 ± 0.01

Table S3: Secondary structure analysis of the illustrative conformations of the most-populated microstates of hIAPP and hIAPP-NS8.

System	Microstates	helix[a]	β-sheet[b]	bend	turn	coil
hIAPP	m_1	32	22	11	16	19
	m_2	35	0	14	32	19
	m_3	32	5	19	17	27
hIAPP-NS8	m_1	35	0	14	23	28
	m_2	38	5	9	22	26
	m_3	38	0	14	20	28

[a] helix= 3_{10} + α + π helix; [b] β-sheet= β-strand + β−bridge